Journal of Hazardous Materials, 34 (1993) 31–50
Elsevier Science Publishers B.V., Amsterdam

Field-scale rotary kiln incineration of batch loaded toluene/sorbent. II. Mass balances, evolution rates, and bed motion comparisons

Christopher B. Leger[a], Charles A. Cook[a], Vic A. Cundy[a,*], Arthur M. Sterling[b], Alfred N. Montestruc[a], Allen L. Jakway[a] and Warren D. Owens[c]

[a] *Mechanical Engineering Department and* [b] *Chemical Engineering Department, Louisiana State University, Baton Rouge, LA 70803 (USA)*
[c] *Mechanical Engineering Department, The University of Utah, Salt Lake City, UT 84112 (USA)*

(Received August 23, 1992; accepted in revised form December 14, 1992)

Abstract

A field-scale rotary kiln incinerator is used to obtain data on the processing of toluene contaminated sorbent contained in plastic packs. The solids bed in the kiln exhibited slipping motion during these experiments. Evolution rates for toluene are determined from experimental data, and cumulative evolution curves are generated. These cumulative evolution curves are very nearly approximated by an exponential function, and as such can be characterized by an exponential time constant. The average time constant for toluene evolution is 141 seconds. This time constant is not dependent upon either kiln rotation rate or turbulence air addition. Unmetered air infiltration was calculated to be between 2.8 and 3.5 times the metered air flow rates. Mass balances on the toluene are performed, yielding good results which are also independent of experimental conditions. The data suggest that stack oxygen concentrations and stack flow rates may be the preferred data for these purposes because they are monitored in existing rotary kiln incinerator facilities. A comparison of contaminant evolution during slipping and slumping bed motion is also discussed.

Introduction

An extensive study of an industrial scale rotary kiln incinerator is being conducted by a team of researchers from Louisiana State University and the University of Utah. The focus of the study is a 17 MW rotary kiln incinerator operated by the Louisiana Division of The Dow Chemical Company, in Plaquemine, LA. This facility has been described in several previously reported studies [1–6]. The experimental details of the most recent study

* To whom correspondence should be addressed.

described here, as well the entire data set obtained during this study, were presented by Leger et al. [7, 8]. In these experiments the kiln rotation rate was either 0.1 rpm or 0.25 rpm (slow or fast, respectively), and the kiln was operated with or without the addition of turbulence air (compressed air injected in the front of the kiln to induce mixing and swirl). The four experimental conditions (fast, turbulence air off; fast, turbulence air on; slow, turbulence air on; slow, turbulence air off) were repeated on a second day of testing. During each experimental condition, six plastic packs containing toluene-contaminated clay sorbent were incinerated, one every ten minutes. The transient responses measured throughout the incinerator system for the six packs were ensemble averaged to produce an average response for a single pack under each operating condition. These averaged responses are presented in a companion paper [8].

In previous studies [9, 10] continuous gas analyzers were used to monitor conditions only at the kiln exit. Contaminant evolution rates and mass balances were performed using these data, although some very restrictive assumptions were necessary. The primary difficulty was the use of measurements from only two points at the kiln exit to predict the overall species flow rates even though large gradients in species concentrations and temperature are known to exist there. A system of weighting factors was developed to assign a fraction of the overall flow to the concentrations measured at each probe location. Using these methods, mass balances obtained during operation without turbulence air were quite good. When turbulence air was added to the system, however, the mass balances were not as good.

From the previous work it became clear that measurements taken at the kiln exit, although informative, were not sufficient for calculating contaminant evolution rates and closing mass balances without making gross assumptions. The poor mixedness of the gas stream at the kiln exit does not allow one to calculate accurately the total flow rate of a species without measuring both the species concentration and the gas velocity at numerous locations over the exit cross-section. Otherwise, only gross assumptions about the species and flow distribution can be made. The need for better data with which to calculate contaminant evolution rates was one of the motivations for adding continuous measurements of O_2 and CO_2 in the afterburner and O_2 in the stack. The assumption of a well-mixed gas stream characterized by a uniform concentration of each gas species seems much more realistic at these locations. Measurements taken at a single location can then be used to calculate contaminant evolution rates and close mass balances without resorting to complicated weighting factor schemes. Thus, the techniques used in this work are similar to those used in the previous mass balance work, except for the use of different monitored variables and less restrictive assumptions.

In this paper, the averaged data from the companion paper [8] are used, together with input air and natural gas flow rates, to calculate the average leak air flow rates and the time dependent toluene evolution rates. Using these results, mass balances are performed and the characteristic times for toluene

evolution are determined. The first step in this process is to determine the baseline O_2 and CO_2 concentrations in the afterburner and the baseline O_2 concentration in the stack. These, together with the metered natural gas and air flow rates into the system, are then used to calculate the rate of air leakage into the system. The total air and natural gas flow rates, together with the stoichiometric equation for methane and air combustion, are used to calculate the total flow rate of combustion gas through the system (from the afterburners to the stack). Then, using the combustion stoichiometry of toluene and air, and the deviation of the O_2 and CO_2 concentrations from baseline, the time resolved toluene combustion rates are calculated. Integrating the toluene combustion rate over time, a mass balance on toluene is performed for the system. Using the cumulative toluene evolution curve, a characteristic time for the evolution process is determined. The toluene evolution rate curves are compared to the xylene evolution rate curves obtained earlier [9], and the differences, presumably caused by the different types of bed motion, are discussed. Finally, the implications of this work are summarized.

Baseline estimation and flow rate determination

The first step in calculating toluene evolution rates and performing toluene mass balances is to establish the gas flow rates in the system. Incinerator systems operate at a slight vacuum to prevent fugitive emissions; this causes unmetered air infiltration. Because air leakage into the system is not known explicitly, the flow rates must be established from experimental measurements of the baseline combustion products. The term "baseline" refers to the steady conditions existing in the incinerator system without any contaminant or pack combustion. The baseline levels of CO_2 and O_2 measured in the afterburner and stack are produced only by the natural gas and air introduced into the kiln and afterburner. Even when combustion of toluene perturbs these concentrations, they return to the baseline levels before the next pack is inserted. Figure 1 shows a typical ensemble averaged CO_2 trace from the afterburner. The peak in CO_2 due to toluene combustion is seen, as well as a drop in CO_2 mole fraction below baseline shortly before the combustion begins. This drop in CO_2 corresponds with the opening of the loading chute door in the kiln to insert the pack and the resulting inrush of leak air above the baseline flow rate. Although a double-door system is used during the loading process, the seal is imperfect. The CO_2 mole fraction approaches the baseline level before the loading chute door is opened, and it is seen to resume momentarily the baseline value after the loading chute door closes, but before toluene combustion begins. For this work, the baseline mole fraction of CO_2 or O_2 is the average of the values exhibited immediately before the loading chute door opens and immediately before pack combustion begins. This value is determined by first graphing the data, drawing a best estimate horizontal line through the data immediately before and after the loading chute door perturbation, and reading

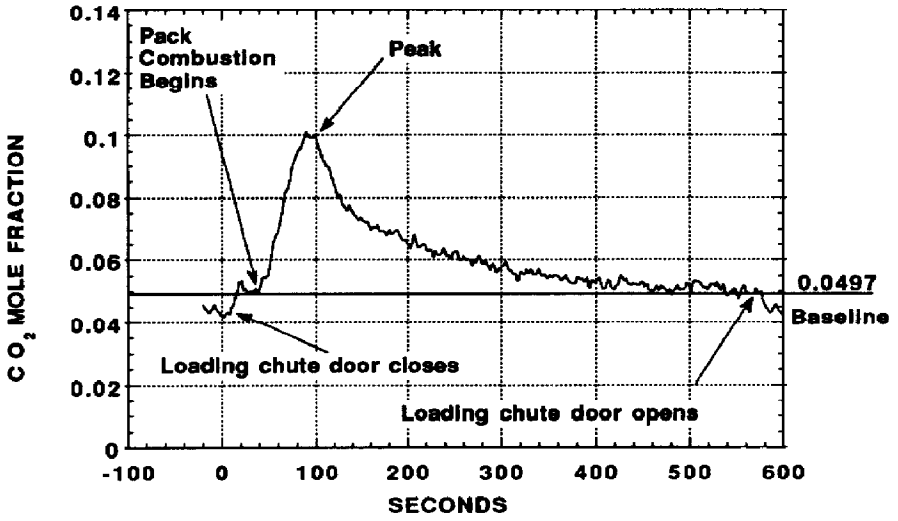

Fig. 1. Typical averaged CO_2 response curve showing important features and baseline. The data were obtained on 3 October 1990 during fast kiln rotation rate with no turbulence air addition.

the coordinate of this line from the vertical axis in terms of mole fraction. This line and the corresponding value are also shown in Fig. 1. Although this is a manual procedure, it is the most reliable method available and it is not entirely arbitrary thanks to the presence of the loading chute door perturbation that is used as a marker.

The following assumptions are made in determining the baseline air leak rate and the total flow rate:

1. The natural gas is assumed to be pure CH_4.
2. The CH_4 undergoes complete combustion with air, providing baseline levels of O_2 and CO_2 against which transients due to toluene combustion can be measured.
3. Combustion of all toluene in a pack is completed before the next pack is inserted 600 seconds later, so that baseline O_2 and CO_2 concentrations may be estimated at the beginning and end of each transient response.
4. No air leakage occurs downstream of the afterburner sampling location.
5. Metered air and natural gas flow rates, together with the calculated air leak rate, yield a total flow rate that is constant under baseline conditions. This assumption is known to be incorrect when the loading chute door is open; however, neither baseline values nor toluene evolution rates are calculated during that period of time.
6. The flow at the afterburner and stack locations is homogeneous with respect to the CO_2 and O_2 concentrations under baseline conditions. Thus, the measured concentrations are representative of the entire flow at these locations.

The following derivation is used to calculate the baseline air leak rate and the total flow rate, and the terms are defined in the glossary. The stoichiometry for complete CH_4 combustion with oxygen is given as:

$$CH_4 + 2O_2 \rightarrow CO_2 + 2H_2O \quad (1)$$

The combustion process for the kiln and afterburner together, under baseline conditions, may be represented by the following stoichiometric equation:

$$M_{CH_4}CH_4 + (M_{air} + M_{leak})(0.208O_2 + 0.792N_2) \rightarrow$$

$$M_{CH_4}CO_2 + 2M_{CH_4}H_2O + (M_{air} + M_{leak})(0.208O_2 + 0.792N_2) - 2M_{CH_4}O_2 \quad (2)$$

The total molar dry flow rate after the combustion process is obtained from the right hand side of eq. (2) by summing all coefficients except that for H_2O to yield:

$$M_{dry\ flow} = M_{air} + M_{leak} - M_{CH_4} \quad (3)$$

The dry flow rate is of interest because the instruments used to measure the CO_2 and O_2 concentrations required dry gas samples. From the stoichiometric coefficient for the CO_2 produced in eq. (2), and by using eq. (3) for the total molar flow rate of products, the mole fraction of CO_2 in the products on a dry basis is:

$$[CO_2] = M_{CH_4}/(M_{air} + M_{leak} - M_{CH_4}) \quad (4)$$

Here the bracketed species, $[CO_2]$, indicates dry mole fraction. Solving eq. (4) for the air leak rate yields:

$$M_{leak} = M_{CH_4}(1 + 1/[CO_2]) - M_{air} \quad (5)$$

An alternative approach for determining the air leak rate is to solve eq. (2) in terms of the O_2 mole fraction on a dry basis. The result is:

$$[O_2] = (0.208(M_{air} + M_{leak}) - 2M_{CH_4})/(M_{air} + M_{leak} - M_{CH_4}) \quad (6)$$

Equation (6) is then solved for the air leak rate as:

$$M_{leak} = M_{CH_4}(2 - [O_2])/(0.208 - [O_2]) - M_{air} \quad (7)$$

Equation (5) may be used to calculate the baseline leak rate of air using metered flow rates and the baseline CO_2 mole fraction measured at the afterburner. Equation (7) will also yield the baseline leak rate of air; it can be applied using either the baseline O_2 mole fraction measured in the afterburner or measured in the stack. Regardless of the method used to calculate the leak rate of air, eq. (3) gives the total dry molar flow rate through the system at either the afterburner sampling location or the stack.

Table 1 shows the metered air and natural gas flow rates, as well as the measured baseline mole fractions of CO_2 and O_2 at the afterburner and stack, for each operating condition and date. In the table, the experimental conditions are abbreviated, so that the condition of "fast kiln rotation rate with

TABLE 1

Natural gas and air flow rates, and measured baseline mole fractions of O_2 and CO_2 as a function of experimental conditions (fast or slow kiln rotation rate, turbulence air on or off, data taken on 3, 4 October 1990)

Experimental condition	Natural gas M_{CH_4} [a]	Metered Air M_{air} [a]	$[O_2]$ [b] Afterburner	$[CO_2]$ [b] Afterburner	$[O_2]$ [b] Stack
Fast off 3	840	4200	0.123	0.050	0.132
Fast off 4	870	4480	0.130	0.045	0.127
Fast on 3	1060	6610	0.133	0.043	0.134
Fast on 4	1060	7450	0.136	0.044	0.136
Slow off 3	870	3920	0.116	0.053	0.127
Slow off 4	860	4480	0.125	0.049	0.127
Slow on 3	1060	6570	0.132	0.039	0.134
Slow on 4	1050	7450	0.137	0.040	0.135

[a] Standard cubic meters per hour. To obtain kmol/s, multiply by 1.24×10^{-5}.
[b] Measured baseline mole fraction.

turbulence air off on 3 October 1990" becomes "Fast Off 3". Notice that when the turbulence air is on, the natural gas flow rate is increased, and the metered air flow (which includes both the burner air and the turbulence air) is also increased. This increase in natural gas input is required to heat the added cool turbulence air to maintain the system operating temperature according to the facility thermocouple located at the kiln exit. The values given in Table 1 are those necessary to solve for leak air flow rates using eqs. (5) or (7).

Table 2 shows the leak air flow rate calculated using each approach, and the resulting total flow rate using each leak rate. These total dry flow rate calculations are based upon:

1. Leak rate estimated from baseline afterburner O_2 mole fraction,
2. Leak rate estimated from baseline afterburner CO_2 mole fraction,
3. Leak rate estimated from baseline stack O_2 mole fraction, and
4. Total flow rate correlated from pressure across the induced draft fan at the stack.

Observe that the calculated leak rates are very large; for operation with turbulence air off the leak air flow rate averaged 3.5 times the metered air flow rate, while for operation with turbulence air on the ratio is 2.8. The total dry flow rates calculated from the three leak air flow rates agree rather well; however, the dry flow rate measured across the induced draft fan, even after correction for density and moisture, is generally higher.

Toluene evolution rates

Once the total flow rates and baseline values for O_2 and CO_2 concentrations have been established, the rate of toluene combustion as a function of time may

TABLE 2

Leak air flow rates and total dry flow rates of combustion products as a function of experimental condition and calculation method

Experimental condition	Calculated leak air flow M_{leak}[a]			Calculated total dry flow $M_{dry\ flow}$[a]			Measured Dry flow[e]
	AB[b] O_2	AB[c] CO_2	Stack[d] O_2	AB[b] O_2	AB[c] CO_2	Stack[d] O_2	$M_{dry\ flow}$[a]
Fast off 3	14300	13500	16300	17700	16900	19700	25300
Fast off 4	16200	15600	15500	19900	19200	19100	24900
Fast on 3	19600	19200	20000	25100	24700	25600	29800
Fast on 4	20000	17700	19800	26400	24100	26200	30500
Slow off 3	13900	13300	16100	16900	16300	19200	25000
Slow off 4	14900	13800	15500	18600	17500	19100	25400
Slow on 3	19300	21200	19900	24800	26700	25400	29600
Slow on 4	20300	20000	19500	26700	26400	25900	30700

[a] Standard cubic meters per hour. To obtain kmol/s, multiply by 1.24×10^{-5}.
[b] Based upon baseline afterburner O_2 mole fraction.
[c] Based upon baseline afterburner CO_2 mole fraction.
[d] Based upon baseline stack O_2 mole fraction.
[e] Total dry flow rate correlated from pressure rise across the induced draft fan.

be calculated. The following additional assumptions are necessary before proceeding:

1. The toluene undergoes complete combustion, forming CO_2 and H_2O, and consuming O_2. Concentrations of incomplete combustion products such as CO, hydrocarbons, and soot are negligible.
2. The perturbation of the measured CO_2 and O_2 mole fractions caused by combustion of the plastic pack itself is negligible [7].
3. The flow at the afterburner and stack locations remains homogeneous with respect to the CO_2 and O_2 concentrations during the combustion of toluene in the kiln.
4. The combustion of toluene has only a negligibly small effect on the dry gas flow rate at the afterburner and stack. In other words, the flow rates calculated from baseline conditions remain representative during the combustion of toluene [10].
5. There is no delay between the evolution of toluene from the sorbent and its subsequent combustion, making the evolution rate of toluene equal to the calculated rate of toluene combustion.

The rate of toluene combustion can be calculated from the measured response of the CO_2 mole fraction in the afterburner or the O_2 mole fraction in the afterburner or the stack. The deviation of the CO_2 or O_2 concentrations from baseline values represents the effect of toluene combustion. The

stoichiometry for complete toluene combustion is:

$$C_7H_8 + 9O_2 \rightarrow 7CO_2 + 4H_2O \quad (8)$$

Thus for every mole of toluene burned, 7 moles of CO_2 are formed and 9 moles of O_2 are consumed. On the basis of measured CO_2 mole fraction, we can then express the toluene combustion rate (in kmol/s) as:

$$M_{C_7H_8} = [([CO_2] - [CO_2]_{baseline})M_{dry\ flow}]/(7 \times 3600) \quad (9)$$

Similarly, the toluene combustion rate based upon measured O_2 mole fraction is:

$$M_{C_7H_8} = [([O_2] - [O_2]_{baseline})M_{dry\ flow}]/(9 \times 3600) \quad (10)$$

Note that since the CO_2 and O_2 concentrations were measured as a function of time, eqs. (9) and (10) can be applied to give toluene evolution rates as a function of time.

As seen in Table 2, there are four ways to obtain the total dry flow rate (calculation based upon measured afterburner CO_2 mole fraction, calculation based upon measured afterburner O_2 mole fraction, calculation based upon measured stack O_2 mole fraction, and direct measurement from pressure drop across the induced draft fan). Similarly there are three ways to calculate the toluene evolution rate (based upon the mole fraction response of the afterburner CO_2, afterburner O_2, and stack O_2) once the total dry flow rate is specified. This yields 12 possible combinations of flow rate and species response to calculate toluene evolution rate. To reduce the number of combinations, the flow rate and species response methods were grouped in a logical manner. The same data that were used for the total dry flow rate calculation were also used for the toluene evolution rate calculation. Ultimately, four toluene evolution calculation approaches were compared. They are:

1. The dry flow rate, obtained from eq. (7) using the baseline afterburner O_2 mole fraction, is used in eq. (10) together with the response of the afterburner O_2 mole fraction to obtain the toluene evolution rate.
2. The dry flow rate calculated using eq. (5) from the afterburner CO_2 baseline mole fraction is used in eq. (9) to obtain the toluene evolution rate.
3. The dry flow rate, obtained from eq. (7) using the baseline stack O_2 mole fraction, is used in eq. (10) together with the response of the stack O_2 mole fraction to obtain the toluene evolution rate.
4. The dry flow rate from the induced draft fan measurement is used in eq. (10) together with the stack O_2 mole fraction response to give a fourth estimate of the toluene evolution rate.

Figure 2 shows the resulting toluene evolution rate calculated using method (1) from the CO_2 mole fraction curve shown in Fig. 1. The toluene evolution rate is normalized by the total amount of toluene initially present in a pack. Notice that the time dependent toluene evolution rate curve is directly related to the CO_2 mole fraction curve. Very similar results are obtained using the O_2 concentrations measured in the afterburner and stack. Since the time

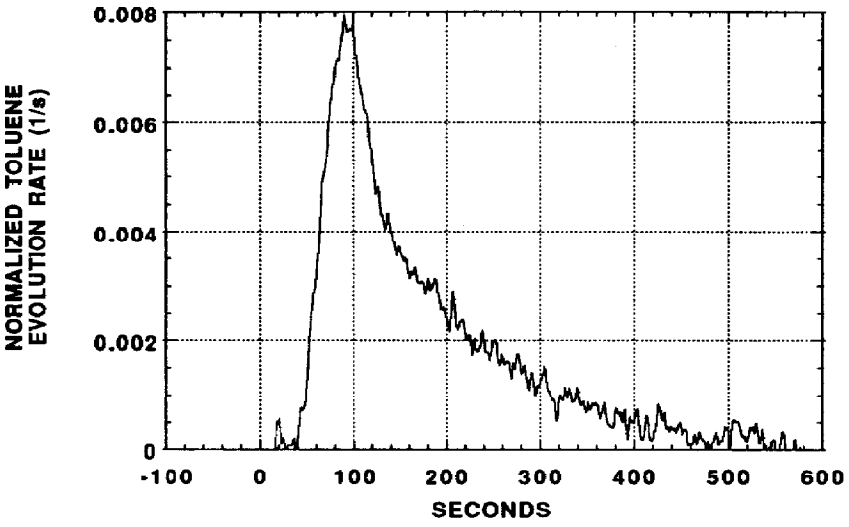

Fig. 2. Normalized toluene evolution rate (with respect to the total amount of toluene initially present in a pack) obtained from the afterburner CO_2 response shown in Fig. 1.

dependent toluene evolution rate curves are intermediate results, they are not all shown. However, the toluene evolution curves obtained from the afterburner CO_2 data are presented later in this paper for comparisons with xylene evolution curves from Lester et al. [9].

Toluene mole closure

Once the instantaneous toluene evolution rates are obtained, the calculation of mole balances on toluene is straightforward. One must simply integrate the toluene evolution rates over time to obtain the cumulative toluene evolution. The toluene evolution rate always return to zero within 600 seconds, so the cumulative toluene evolution should always approach the total moles of toluene initially present in a single pack. The cumulative toluene evolution curves generated from the afterburner CO_2 data and normalized by the total moles of toluene initially present in a pack are shown in Fig. 3. Similar curves were generated based on the afterburner and stack O_2 responses.

Each toluene-laden pack incinerated in the system contained 0.178 kmol of toluene. The final values of calculated cumulative toluene evolution were normalized, dividing by 0.178 kmol to obtain the closure on toluene. This mole closure is expressed as the ratio of calculated toluene evolution to the toluene content of a single pack. The calculated fractional toluene closures are given in Table 3 for each method of calculation and each operating condition. These fractional toluene closures are also shown graphically in Fig. 4 for each calculation method and operating condition. Overall, the toluene closure is

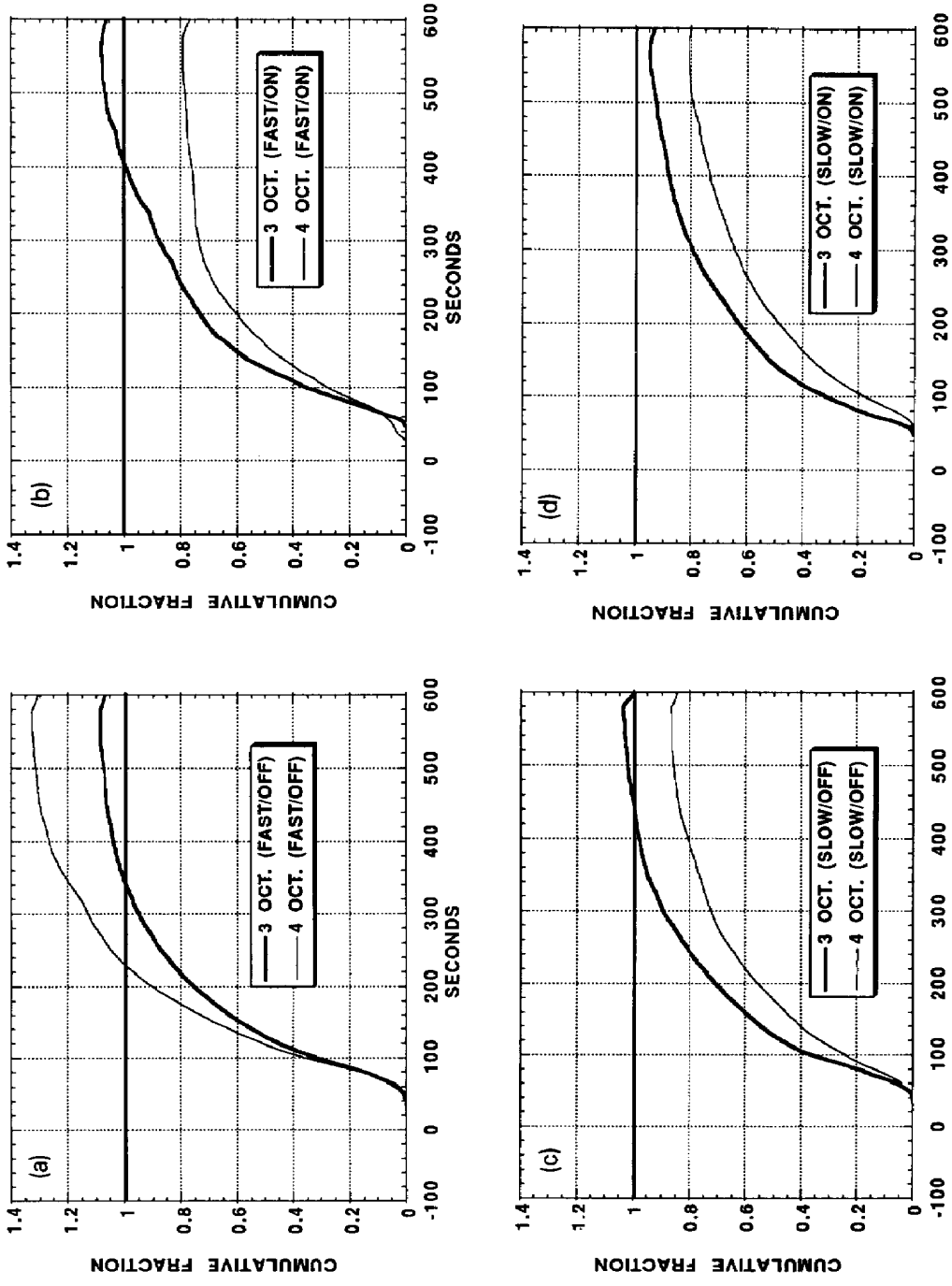

Fig. 3. Normalized cumulative toluene evolution (with respect to the total amount of toluene initially present in a pack) as a function of experimental conditions. Fast kiln rotation (a) without, and (b) with turbulence air (TA). Slow kiln rotation (c) without, and (d) with turbulence air (TA).

TABLE 3

Toluene mass closure fraction obtained for each experimental condition for each calculation method. See also Fig. 4

Experimental condition	Toluene closure				Average	Standard deviation
	AB O_2 [1]	AB CO_2 [2]	Stack O_2 [3]	Stack flow [4]		
Fast off 3	0.90	1.09	0.76	0.98		
Fast off 4	1.13	1.33	0.84	1.10	1.02	0.18
Fast on 3	0.97	1.08	0.88	1.03		
Fast on 4	0.73	0.79	0.92	1.07	0.93	0.13
Slow on 3	0.54	0.95	0.78	0.90		
Slow on 4	0.57	0.81	0.63	0.75	0.74	0.15
Slow off 3	0.80	1.04	0.73	0.95		
Slow off 4	0.79	0.87	0.59	0.79	0.82	0.14
Average	0.80	0.99	0.77	0.95	0.88[a]	
Standard dev.	0.20	0.18	0.12	0.13		0.18[a]

[1] Using the afterburner O_2 mole fraction for total flow rate and toluene evolution rate.
[2] Using the afterburner CO_2 mole fraction for total flow rate and toluene evolution rate.
[3] Using the stack O_2 mole fraction for total flow rate and toluene evolution rate.
[4] Using the total dry flow rate measured in the stack together with the stack O_2 mole fraction to get toluene evolution rate.
[a] Average and standard deviation of all 32 values of toluene closure.

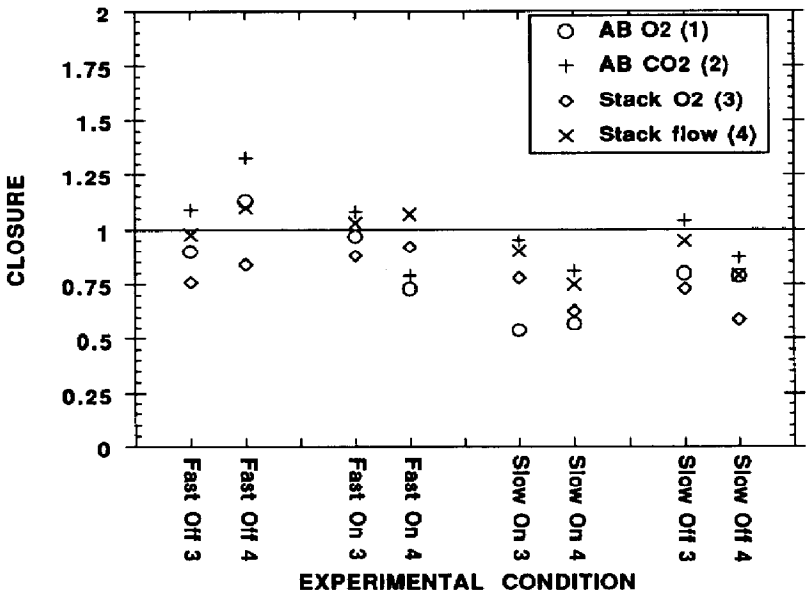

Fig. 4. Mole closures on toluene as a function of operating condition and calculation method. Parenthetical numbers in key correspond with those in Table 3.

quite good considering the nature of these experiments. Table 3 also shows the average toluene closures for each calculation method and experimental condition, and the standard deviation of these values. Based on the data of Table 3, the overall average toluene closure is 88% and the overall standard deviation of the data is 18%. An analysis of variance (ANOVA) test showed that the variation of toluene closure between consecutive days was not statistically significant (99% significance level). The variation in toluene closure as a function of turbulence air addition was also not statistically significant. The variation between calculation methods was significant as was the influence of rotation rate. Although the calculation methods influence closure, the results of one method can not be selected over another. While we intuitively agree that calculation method will have an influence on calculated mass closure, it was unexpected that kiln rotation rate would influence mass closure. Changing the kiln rotation rate from fast to slow caused a decrease in average mass closure from 98% to 78%. The reason for this influence remains unclear.

In earlier studies on xylene and dichloromethane using measurements at the kiln exit only [9, 10], closure was not good during operation with turbulence air addition. Since this dependence was not observed in the current experiments, poor closure with turbulence air addition in previous work may have occurred because the turbulence air influenced the quality of the assumptions used in the analysis and not because the ultimate evolution of each species was reduced.

Characteristic time for evolution

In previous work [9, 10] the time necessary for the contaminant to evolve was characterized by the evolution interval, defined as the time required for the middle 80% of the ultimate contaminant evolution to occur. This definition was used because the cumulative evolution curves tended to be irregular, particularly near the beginning and end, due to pack breakdown and bed motion effects. From Fig. 3 one observes that the shape of the cumulative evolution curve for toluene from a slipping bed is very smooth and repeatable for all the data. In fact, the cumulative evolution curves for toluene shown in Fig. 3 can be closely approximated by an exponential function, with the exponential time constant representing the characteristic time for contaminant evolution. If the cumulative evolution curves of Fig. 3 are normalized by their final values, yielding $N_{C_7H_8}(t)$, the resulting curves will begin at 0, approach 1 at the end, and can be readily fit by the expression:

$$N_{C_7H_8}(t) = 1 - \exp(-t/\tau) \tag{11}$$

Figure 5 shows the application of eq. (11) to fit a typical normalized cumulative evolution curve, with a resulting evolution time constant of 120 seconds.

Since the data have been normalized and only the time constant is being extracted, the results are only dependent upon the species response used. In

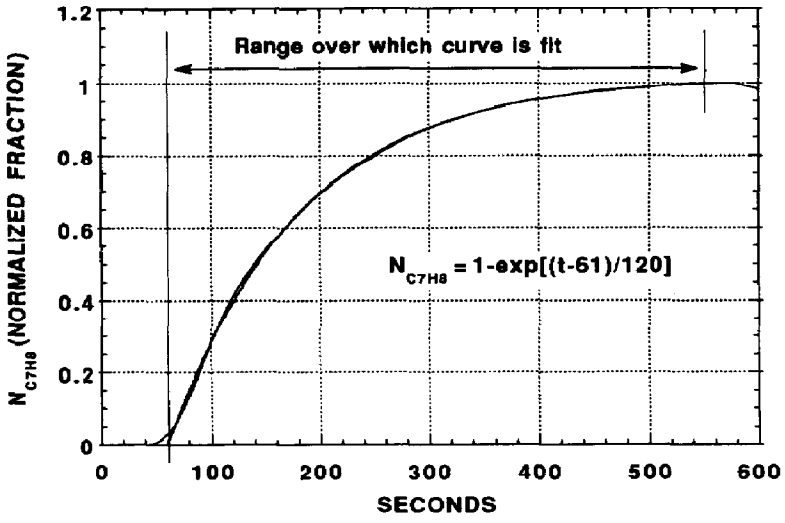

Fig. 5. Typical cumulative evolution curve. The fitted curve follows the data very closely over the range of the fit. Data was obtained on 3 October 1990 from the afterburner CO_2 response at fast rotation with no turbulence air addition (the same data used in Figs. 1 and 2).

other words, differences in the total dry flow rate are normalized out, and there are only three remaining independent normalized evolution rate calculation methods (based upon afterburner O_2 response, afterburner CO_2 response, and stack O_2 response). The cumulative evolution curves obtained from these three methods are fit using eq. (11), and the resulting time constants are given in Table 4 and shown in Fig. 6. Table 4 also shows the averages and standard deviations of the time constants over the four experimental conditions and over the three calculation methods. The overall average time constant for contaminant evolution is 141 seconds, with a standard deviation of 23 seconds. Statistical analysis (ANOVA) showed that the time constants were independent of either the kiln rotation rate or turbulence air addition. This is very different from previous studies on xylene and dichloromethane, where both experimental variables were seen to influence the evolution interval. Figure 6 also shows that the use of stack O_2, afterburner O_2, or afterburner CO_2 in the calculations had no clear effect on the evolution time constant, although the use of afterburner O_2 caused more scatter in the results than did the others.

From the comparisons between calculation methods for obtaining toluene closure and evolution time constants, no single calculation method stands out as clearly better than the others. However, the calculation methods are not equivalent in terms of measurement and calculation difficulty. Measurement of the O_2 and CO_2 concentrations at the afterburner location is far more difficult than at the stack location. Using these measurements to calculate air leak rates is also somewhat troublesome. Furthermore, the total dry flow rate is simply measured at the stack. The simplest method for obtaining toluene

TABLE 4

Evolution time constants for each experimental condition and calculation method. See also Fig. 6

Experimental condition	Time constant (seconds)			Average	Standard deviation
	AB O_2[a]	AB CO_2[b]	Stack O_2[c]		
Fast off 3	137	120	117		
Fast off 4	141	127	143	131	11
Fast on 3	190	140	155		
Fast on 4	116	103	129	139	31
Slow on 3	95	138	162		
Slow on 4	141	160	153	142	25
Slow off 3	157	130	128		
Slow off 4	183	151	158	151	20
Average	145	134	143	141[d]	
Standard dev.	32	18	17		23[d]

[a] From the afterburner O_2 mole fraction response.
[b] From the afterburner CO_2 mole fraction response.
[c] From the stack O_2 mole fraction response.
[d] Average and standard deviation of all 24 values of the time constant.

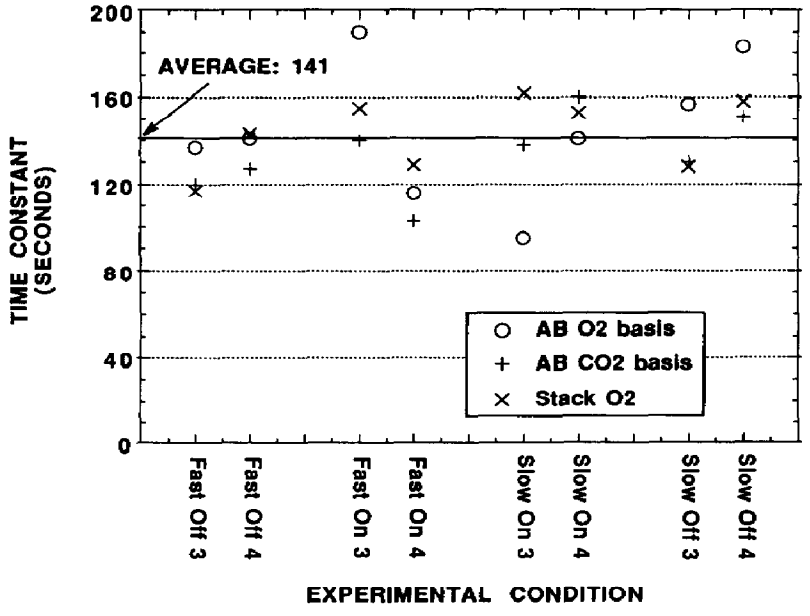

Fig. 6. Evolution time constants as a function of operating condition and originating data. (See Table 4.)

evolution rates, therefore, is to use the stack O_2 measurements together with flow rates obtained from the induced draft fan at the stack (calculation method 4). Capability for obtaining both of these measurements (stack O_2 and stack flow rate) is standard on rotary kiln incinerator facilities since these data are routinely used to certify that the system is operating within permit guidelines. Since the waste evolution rates obtained with these measurements (calculation method 4) are equivalent to those obtained with the other methods, future evolution rate characterization studies could make use of existing facility instrumentation for waste evolution rate calculations.

The effects of bed motion on evolution rate

As discussed in the companion paper [8], the bed of solids was exhibiting slipping motion during the toluene experiments, in contrast to the slumping motion observed previously during the xylene experiments [9]. This difference in bed motion regime is a result of either the presence of a thermocouple in the solids bed, or a change in the surface roughness of the slag-coated rotary kiln walls. In the slumping motion regime, solids intermittently tumble down the free surface of the bed, and then follow the wall in a layer below the surface before reemerging to tumble across the surface again. This motion causes the solids to mix, and each part of the bed is repeatedly exposed at the surface. During the toluene experiments, the bed exhibited a slipping motion. With this type of motion, the entire bed slips relative to the wall, and it essentially moves as if it were a solid piece, with the same particles remaining on the surface. In the slipping bed motion regime, the solids mix very slowly. The differences in the bed motion regimes preclude the use of this toluene data in the scaling analysis presented by Lester et al. [9] as was originally intended. It does, however, allow a comparison of evolution characteristics between slipping and slumping beds. Toluene and xylene have similar physical and combustion characteristics, and the experimental conditions were very similar for each contaminant. Since the only major difference between the experiments was the bed motion, comparisons between the xylene and toluene evolution behavior should show the influence of bed motion.

The toluene and xylene evolution rate data are shown in Fig. 7 for the four operating conditions. The normalized toluene evolution rates obtained from the afterburner CO_2 are shown. Each graph also contains the normalized xylene evolution rate obtained from ensemble averaged CO_2 measurements at the kiln exit using CO_2 weighting factors [9]. All the evolution curves are normalized so that the integral of the curve over time is unity.

The toluene data show good overall repeatability between the duplicate tests at each operating condition, although the magnitude of the initial spike in evolution shows some variation. For all operating conditions, the toluene evolution curves show essentially the same behavior: a quick rise to the maximum followed by a gradual decay back to the baseline. In contrast, the

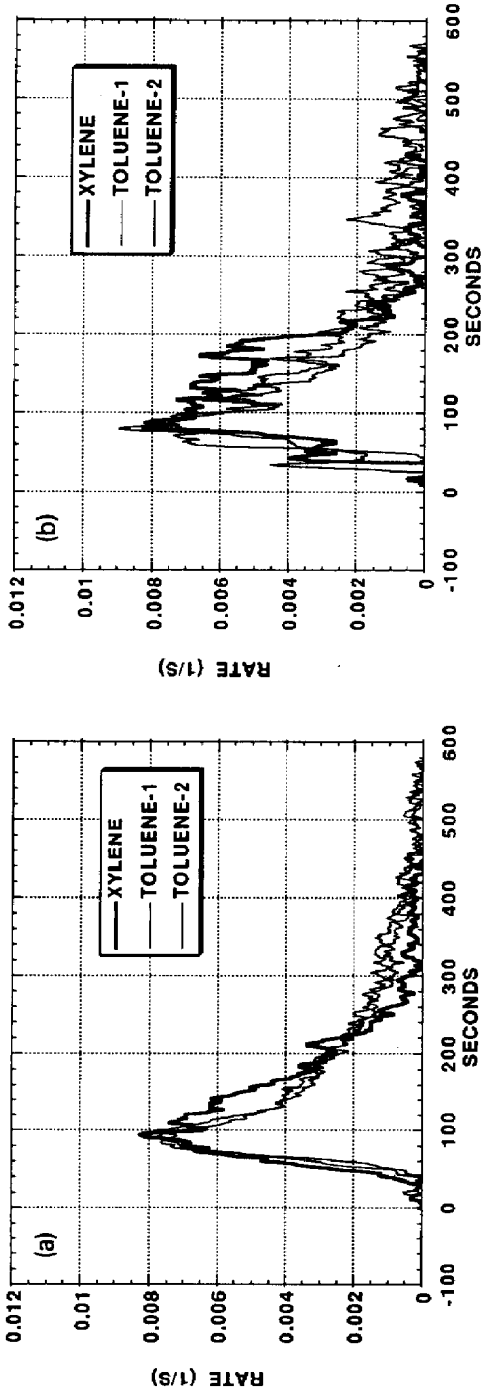

Fig. 7. Comparison of normalized evolution rates for slipping bed (toluene from this study) and a slumping bed (xylene from Lester et al. [9]). For the toluene, replicates obtained from 3 and 4 October 1990 are included (thin lines). Fast kiln rotation (a) without, and (b) with turbulence air. Slow kiln rotation (c) without, and (d) with turbulence air.

xylene evolution curves show a broader maximum followed by a rapid decline. Also, the xylene data show a marked difference between fast and slow kiln rotation rates, with the slow rotation rate resulting in a much broader, less intense period of evolution. The xylene data for the slow rotation rate show three distinct evolution peaks in each case, with a separation of approximately 80 seconds between the peaks. This separation appears to correspond with the time necessary for a particle to circulate through the bed and return to the surface. None of this behaviour is observed in the toluene evolution data.

From the comparisons between evolution for a slipping bed and a slumping bed, some practical observations can be made. First, the evolution behavior observed from the slumping bed is generally better from a kiln operational perspective because of the broader, less intense waste evolution, with less propensity for causing transient "puffs", as defined by Linak et al. [11]. This difference in evolution behavior may be caused primarily by the action of the hot, clean sorbent material present in the kiln from previous packs. During slumping bed motion, the preexisting bed material repeatedly buries the fresh charge from a new pack. This appears to cause an increased resistance to mass transfer from the buried charge, and possibly reduces the rate of heat transfer to the buried charge as well, resulting in a decline in evolution rate. When the fresh charge is reexposed due to circulation of the bed, the evolution rate increases again. This is in contrast to the slipping bed case, where apparently the fresh charge is never buried by preexisting bed materials but rather lies on top of these materials. For volatile wastes such as toluene and xylene, the slipping bed motion is much less preferable because it causes higher peak evolution rates which could, if the magnitude is great enough, lead to a transient "puff". However, if the waste is much less volatile or if it is present in low concentrations, a slipping bed motion may be acceptable because rapid evolution of the waste is unlikely. For these wastes, a slipping bed motion may even be advantageous because the contaminated solids do not become buried in the bed, and so could theoretically be cleaned of their hazardous components more rapidly.

Leger et al. [8] observe that the type of bed motion exhibited may be controllable by the drag exerted by stationary protuberances extending into the bed, or by controlling the roughness of the kiln's inner walls. In addition to hazardous waste, this has important implications in remediation of contaminated soil in rotary-type units. Depending on the level of contamination, moisture content, and the soil type, one bed motion may be preferred to another. This study has shown that, to some degree, control over the bed motion may be possible using techniques not previously considered. More extensive work is needed to better characterize the controllability of bed motion and its effects on a variety of waste/soil materials in field-scale rotary units.

Summary and conclusions

In this study, a field-scale rotary kiln incinerator is used to obtain data on the processing of toluene contaminated sorbent contained in plastic packs. The

incinerator is probed in several different locations with instruments which continuously monitor species concentrations, temperatures, and pressures. Visual observations indicate that the bed exhibited slipping motion during these experiments. Evolution rates for toluene are determined from experimental data, and cumulative evolution curves are generated. These cumulative evolution curves are very nearly approximated by an exponential function, and as such can be characterized by an exponential time constant. The time constants for toluene evolution average 141 seconds and are not dependent upon either kiln rotation rate or turbulence air addition. Air leak rates into the system are calculated to be between 2.8 and 3.5 times the metered air flow rates. Mass balances on the toluene yielded good results, although slower kiln rotation rate appears to decrease the mass closure. Evolution time constants and toluene closure calculations were comparable regardless of the calculation method used. This suggests that stack oxygen concentrations and stack flow rates may be the preferred data for these purposes because they are monitored in existing rotary kiln incinerator facilities.

Comparisons with evolution data taken previously suggest that the slipping bed motion exhibited during these toluene tests caused the toluene evolution rate (as measured by the evolution time constant) to be independent of kiln rotation rate. The slumping motion exhibited during earlier xylene tests apparently restricted mass transfer thus causing the xylene evolution to occur over a longer time with lower peak evolution rates. From an operational perspective, the slumping motion may be preferable for high concentration volatile wastes because it results in a more steady waste evolution. However, for low volatility wastes or low concentration wastes, the slipping bed motion may be advantageous by reducing the mass transfer resistance thus reducing the time to remove the waste from the solids. More work needs to be done to address these possibilities.

Acknowledgements

The research described in this article has been funded in part by the U.S. EPA through Cooperative Agreement No. CR809714010 granted to the Hazardous Waste Research Center of the Louisiana State University. Although this research has been funded by EPA, it has not been subjected to Agency review and therefore does not necessarily reflect the views of the Agency and no official endorsement should be inferred.

The authors gratefully acknowledge the assistance and cooperation of the Louisiana Division of Dow Chemical USA located in Plaquemine, Louisiana. In particular, the assistance of Tony Brouillette, Jonathan Huggins, Marvin Cox, Darryl Sanderson, and J.J. Hiemenz is appreciated. Although this research has been undertaken in a cooperative nature with Dow Chemical USA, it does not necessarily reflect the views of the Company and therefore no endorsement should be inferred.

The support offered by L.J. Thibodeaux and David Constant, Director and Associate Director respectively, of the Louisiana State University Hazardous Waste Research Center is appreciated. Matching funds from the Mechanical and Chemical Engineering Departments of Louisiana State University have helped to provide needed support. The guidance of Thomas Lester in the foundation and planning of this project is appreciated. The authors gratefully acknowledge the fellowship assistance from the National Science Foundation for one author (Christopher B. Leger) and from the State of Louisiana for two others (Allen L. Jakway and Charles A. Cook). The capable assistance of Roger Conway, Chao Lu, and Dan Farrell is also acknowledged.

Nomenclature

CH_4, O_2, CO_2, H_2O, C_7H_8	methane, oxygen, carbon dioxide, water, and toluene species, respectively, used in stoichiometric equations.
$[O_2]$, $[CO_2]$	measured mole fraction of oxygen and carbon dioxide on a dry basis as a function of time.
$[O_2]_{baseline}$, $[CO_2]_{baseline}$	measured mole fraction of oxygen and carbon dioxide on a dry basis under baseline conditions (no waste combustion).
M_{CH_4}	metered molar flow rate of methane into the kiln and afterburner. (kmol/s)
M_{air}	metered molar flow rate of air into the kiln and afterburner. (kmol/s)
M_{leak}	molar flow rate of air leaking into the kiln and afterburner. (kmol/s)
$M_{dry\ flow}$	total molar flow rate of all product species except water. (kmol/s)
$M_{C_7H_8}$	molar flow rate of toluene evolution from the sorbent. (kmol/s)
$N_{C_7H_8}(t)$	molar evolution rate of toluene at time t, normalized by 0.178 kmol. (1/s)

References

1 V.A. Cundy, T.W. Lester, J.S. Morse, A.N. Montestruc, C. Leger, S. Acharya, A.M. Sterling and D.W. Pershing, Rotary kiln incineration I. An in depth study — Liquid injection, J. Air Pollut. Control Assoc., 39(1) (1989) 63–75.

2 V.A. Cundy, T.W. Lester, A.N. Montestruc, J.S. Morse, C. Leger, S. Acharya and A.M. Sterling, Rotary kiln incineration III. An in depth study — CCl_4 Destruction in a full-scale rotary kiln incinerator, J. Air Pollut. Control Assoc., 39(7) (1989) 944–952.

3 V.A. Cundy, T.W. Lester, A.N. Montestruc, J.S. Morse, C. Leger, S. Acharya and A.M. Sterling, Rotary kiln incineration IV. An in depth study — Kiln exit and transition section sampling during CCl_4 processing, J. Air Pollut. Control Assoc., 39(8) (1989) 1073–1085.

4 V.A. Cundy, T.W. Lester, C.B. Leger, A.N. Montestruc, G. Miller, S. Acharya, A.M. Sterling, J.S. Lighty, D.W. Pershing, W.D. Owens and G.D. Silcox, Rotary kiln incineration — Combustion chamber dynamics, J. Hazardous Mater., 22(2) (1989) 195–219.
5 V.A. Cundy, T.W. Lester, A. Jakway, C.B. Leger, C. Lu, A.N. Montestruc, R. Conway and A.M. Sterling, Incineration of xylene/sorbent packs — A study of conditions at the exit of a full-scale industrial incinerator, Environ. Sci. Technol., 25(2) (1991) 223–232.
6 V.A. Cundy, C. Lu, C.A. Cook, A.M. Sterling, C.B. Leger, A.L. Jakway, A.N. Montestruc, R. Conway and T.W. Lester, Rotary kiln incineration of dichloromethane and xylene — A comparison of incinerability characteristics under various operating conditions, J. Air Waste Manag. Assoc., 41(8) (1991) 1084–1094.
7 C.B. Leger, V.A. Cundy, A.M. Sterling, A.N. Montestruc and A.L. Jakway, Rotary kiln incineration of toluene on sorbent contained in plastic packs — System dynamics inferred from continuous O_2 measurements, Remediation, 1(3) (1991) 275–291.
8 C.B. Leger, V.A. Cundy, A.M. Sterling, A.N. Montestruc, A.L. Jakway and W.D. Owens, Field-scale rotary kiln incineration of batch loaded toluene/sorbent-I: Data analysis and bed motion considerations, J. Hazardous Mater., 34 (1993) 1–29.
9 T.W. Lester, V.A. Cundy, A.M. Sterling, A.N. Montestruc, A. Jakway, C. Lu, C.B. Leger, D.W. Pershing, J.S. Lighty, G.D. Silcox and W.D. Owens, Rotary kiln incineration: Comparison and scaling of field-scale and pilot-scale contaminant evolution rates from sorbent beds, Environ. Sci. Technol., 25(6) (1991) 1142–1152.
10 C.A. Cook, V.A. Cundy, A.M. Sterling, C. Lu, A.N. Montestruc, C.B. Leger and A.L. Jakway, Estimating dichloromethane evolution rates from a sorbent bed in a field-scale rotary kiln incinerator, Combust. Sci. Technol., 85(1–6) (1992) 217–241.
11 W.P. Linak, J.D. Kilgore, J.A. McSorley, J.O.L. Wendt and J.E. Dunn, On the occurrence of transient puffs in a rotary kiln incinerator simulator: I. Prototype solid plastic wastes, J. Air Pollut. Control Assoc., 37(1) (1987) 54–65.